# Metric features of self-organized criticality states in sandpile models

Mario Casartelli†‡ and Massimo Zerbini‡

† Dipartimento di Fisica dell'Università, Parco Area Scienze 7a, 43100 PR, Italy
‡ Instituto Nazionale di Fisica della Materia, Parma, Italy

E-mail: `casartelli@fis.unipr.it`

**Abstract.** A new characterization of self-organized criticality (SOC) states is developed by using metric features of the configuration's space. Quantities mainly referring to the partition formalism, as mutual factorization, Shannon entropy and Rohlin distances with their distributions and power spectra, are considered. Time series for these observables give account of geometrical and dynamical complexity through the interdependence of fractality and flicker noise. For Bak–Tang–Wiesenfeld and Manna automata, new indicators enforce previous results given by standard parameters and allow a deeper insight into the structure of SOC configurations and their time behaviour. Moreover, we obtain indications regarding a possible split in the universality class of the two automata.

Much attention has been devoted in recent years to the characterization of the so-called 'self-organized criticality' (SOC), in order to obtain clear criteria to classify systems such as sandpile automata in the framework of geometro–dynamical complexity. We simply remind the reader here that the critical state is an attractor lacking any characteristic time or length scale. Usual descriptions refer to parameters such as the number of topplings $s$, the amplitude of avalanches $a$ and the avalanches' lifetime $T$ [1–3]. These parameters, which will be precisely recalled below, exhibit power law distributions, i.e., by adopting notations of [3]:

$$P(x) \propto x^{-\tau_x} \tag{1}$$

where $x$ may be $s$, $a$, $T$, and $\tau_x$ is the corresponding exponent used in classifying the model.

The suspicion that a strict interdependence of geometry and dynamics (fractality versus flicker noise) is particularly relevant for these systems was raised from the very beginning of studies on SOC [1]. Now, parameters $s$, $a$ and $T$ obviously depend on the evolving configurations, but the geometrical peculiarity of the SOC regime remains implicit for them: fractality, for instance, does not appear directly in the evolution of cluster shapes, but only through the probability distributions (1). The approach we propose here explicitly refers to the geometrical features of the SOC states in their relations to dynamics, by a suitable metrization of the configuration's sequence. In order to compare the evolving states, we need to introduce a distance between configurations along the trajectory.

For cellular automata, or more generally for discrete systems whose $N$ sites assume numerical values, there is a standard way to introduce a distance through the Hamming functional $\rho_H$, defined by

$$\rho_H(a, b) = \frac{1}{N} \sum_{i=1}^{N} |x_a(i) - x_b(i)| \tag{2}$$

where $x_a(i)$ and $x_b(i)$ denote the values of the site $i$ in the configurations $a$ and $b$ respectively. The advantage of this distance, besides its simplicity, is that it does not care for lattice dimension or symmetries. Actually, it could also be introduced on a graph. However, not only does it require that the value's range, i.e. the alphabet, is numerical, but it is also insensitive to the configuration's shape: the maximum, for instance, is reached for every couple of complementary configurations, independently of their shapes. Moreover, it is not difficult to provide examples of configurations $a, b, c \dots$ having $\rho_H(a, b) = \rho_H(a, c) = \cdots$, but very different value distributions. Consider, e.g., three configurations of a $4 \times 4$ lattice:

$$a = \begin{bmatrix} 1 & 1 & 2 & 2 \\ 1 & 1 & 2 & 2 \\ 1 & 1 & 2 & 2 \\ 1 & 1 & 2 & 2 \end{bmatrix} \qquad b = \begin{bmatrix} 1 & 1 & 2 & 2 \\ 1 & 1 & 2 & 2 \\ 2 & 2 & 1 & 1 \\ 2 & 2 & 1 & 1 \end{bmatrix} \qquad c = \begin{bmatrix} 1 & 2 & 1 & 2 \\ 2 & 1 & 2 & 1 \\ 1 & 2 & 1 & 2 \\ 2 & 1 & 2 & 1 \end{bmatrix}. \tag{3}$$

Clearly, $\rho_H(a, b) = \rho_H(a, c) = \rho_H(b, c) = \frac{1}{2}$. Thus, at least in principle, it seems that the Hamming distance cannot describe the geometrical complexity of value distributions.

A complementary approach, therefore, should stress the metric role of cluster shapes independently of the actual values (numerical or otherwise) on sites. This may be done using the Rohlin distance (see, e.g., [4]), as proposed in [5,6] for general discretizable systems. This distance has already been used to characterize the magnetic transition in automata with Q2R or Metropolis evolution rules, simulating Ising systems in the microcanonical or canonical descriptions respectively [6].

We summarize the formalism and the notation of [6], which immediately fit the needs of every automaton on a square lattice.

Let $a, b, c$, etc be the states, or configurations, of a square lattice $M$ of $N = L \times L$ sites, where every site can assume values in an alphabet $K$: therefore, the configuration's space $\mathcal{S}$ is $K^N$. Consider the dual lattice $M'$: sites of $M$ are now the centres of squares. There is an isomorphism between $M$ and $M'$. Since every site of $M$ is the centre of a square, and every square is labelled by an alphabetic value, every configuration in $M$ is also a configuration of the dual lattice, and we may assume that the configurations' space is the same. Then, the Peierls–Griffith clusterization [7] consists in grouping together, in a single cluster, squares with the same value in $K$ which are connected by a continuous path. Therefore, every cluster is a connected (but, in general, not simply connected) subset of $M'$. For every configuration, these clusters define a finite partition of $M'$, i.e. an exhaustive collection $\alpha$ of disjoints subsets $A_1, A_2, \dots, A_m$ of $M'$, called *atoms* of $\alpha$. A probability in $M'$ is defined by assigning to every atom a measure, $\mu(A_k)$, given by the number of squares in the corresponding cluster divided by $N$. This procedure defines a map $\Phi : \mathcal{S} \to \mathcal{Z}$, where $\mathcal{Z}$ is the set of all the finite measurable partitions of $M'$. Then, the Rohlin distance between two partitions $\alpha$ and $\beta$ in $\mathcal{Z}$ is the functional

$$\rho_R(\alpha, \beta) = H(\alpha|\beta) + H(\beta|\alpha) \tag{4}$$

where $H(\alpha|\beta)$ is the conditional Shannon entropy of $\alpha$ with respect to $\beta$. Note that, for configurations in example (3), we have

$$\rho_R(\alpha, \beta) = \log 2 \qquad \rho_R(\alpha, \gamma) = 3\log 2 \qquad \rho_R(\beta, \gamma) = 2\log 2$$

where, of course, $\alpha = \Phi(a), \beta = \Phi(b), \gamma = \Phi(c)$.

In [6] there is a complete description of the 'reduction process'

$$\pi : (\alpha, \beta) \to (\alpha', \beta')$$

between two partitions $\alpha, \beta$, which defines a new couple $\alpha', \beta'$, where common factors (i.e. subpartitions) have been eliminated as far as possible. A reduced couple $(\alpha', \beta')$ is irreducible, i.e. $\pi^2 = \pi$: the reduction process is a projection on the set of irreducible couples.

The subtle point in this process consists in properly defining the factorization of partitions. Indeed, the whole procedure recalls the elimination of common factors in fractions, and reduced couples are the equivalent of rational numbers. But, for partitions, there is not a uniquely defined factorization in 'prime factors'. The role of prime factors is played by dichotomic (i.e. two-atom) subpartitions. For two-dimensional lattices, the correct dichotomic factors are subpartitions defined by the *external* border of every atom. It holds that $\rho_R(\alpha, \beta) \leqslant \rho_R(\alpha', \beta')$, and the reduced distance $\hat{\rho}_R$ is then defined as

$$\hat{\rho}_R(\alpha, \beta) = \rho_R(\alpha', \beta'). \tag{5}$$

Both $\rho_R$ and $\hat{\rho}_R$ give a quantitative estimate of the non-similarity between $\alpha$ and $\beta$, or $\alpha'$ and $\beta'$. The 'amplification factor' $A$ is defined as

$$A = \frac{\hat{\rho}_R}{\rho_R} = \frac{\rho_R(\alpha', \beta')}{\rho_R(\alpha, \beta)} \tag{6}$$

where it is an index of the *exact* overlap of border paths of atoms in two partitions, and, indirectly, of the local mobility of the clusters. The reduction process, based on the storage and comparative analysis of all borders, requires a heavy computational charge. In the following, couples of partitions will correspond to configurations in consecutive steps during the evolution of the system.

Even if the method may be easily applied to every kind of two-dimensional system, hereafter, to be more specific, we shall refer to sandpile automata, in particular to the Bak–Tang–Wiesenfeld (BTW) and to the Manna models, (see, e.g., [1, 2]). We briefly recall the rules:

- BTW model: every site $(i, j)$ assumes integer values representing the height $h_{ij}$ of a sandpile. Sites are increased by random addition of single grains. There is a critical height $h^c = 3$, and when $h_{ij} > h^c$ there is a distribution of sand grains from the site $(i, j)$ to its next neighbours $\langle ij \rangle$, i.e. $h_{ij} \rightarrow h_{ij} - 4$ and $h_{\langle ij \rangle} \rightarrow h_{\langle ij \rangle} + 1$; this process is said to be toppling;
- Manna model: the same as in BTW, except that $h^c = 1$, and the toppling rules are $h_{ij} \rightarrow h_{ij} - 2$, and only two next neighbours (randomly selected) are increased by 1.

Of course, topplings may propagate until the system reaches a new stable state, and this propagation is called 'avalanche'. In both cases the random addition of sand grains is stopped during the avalanche. An 'internal step' of the avalanche is the refreshing of the whole lattice according to the rule when at least one site is greater than $h^c$. The standard parameters to consider are the number of topplings $s$, the number of internal evolution steps $T$, and the size of the avalanche cluster $a$. Borders are open, and may dissipate sand. In stable states, the only ones considered in cluster formation, the alphabet for BTW is $K = \{0, 1, 2, 3\}$ and for Manna is $K = \{0, 1\}$. Indeed, the values over the critical heights appear only in the intermediate phases of evolution, and do not influence the actual shapes of the atoms we shall consider.

Another interesting quantity is the mean steepness $\bar{v}$, defined by

$$\bar{v} = \frac{1}{N} \sum_{ij=1}^{L} \sum_{\langle ij \rangle} \frac{|h_{ij} - h_{\langle ij \rangle}|}{4}. \tag{7}$$

It is an index of smoothness, measured along the cluster borders.

The analysis will proceed in the following way: starting from an initial configuration $a(0)$, we consider the sequence $\{a(t)\}$ of configurations taken at discrete times $t$. In correspondence to the sequence $\{a(t)\}$, there is a partition sequence $\{\alpha(t)\}$, where $\alpha(t) = \Phi(a(t))$. Discrete times $t$ are the beginning steps of avalanches (in other words, $t$ is the order label of

avalanches). The time discretization, depending on the avalanches' lifetime $T$, is therefore highly dishomogeneous with respect to the 'clock time' defined by the evolution rules. When necessary, we shall also consider single evolution steps (internal and/or external to the avalanches) as given by the rules. For distances, it would have been natural to consider, as relevant partitions, the first and the last ones of every avalanche: however, since the evolution steps between two avalanches modify in most cases one or two sites, the difference with respect to our choice is very small, and practically insignificant on the values of all time series.

In actual simulations, the length of these sequences (i.e. the number of avalanches) reaches $t = 100\,000$, with checks up to $t = 200\,000$, for $L = 50, 100, 200$. We stress that these low values of $L$ depend on the heavy computational charge due to the partitions handling, in particular to the reduction process which requires the factorization of all couples of partitions. The transient time necessary to pass from an initial random configuration to the stable SOC state is around 1000 avalanches for $L = 100$. Our time $t = 0$ starts from the stabilization in the SOC regime.

The time series or quantities we shall consider are as follows:

(1) $\{H(t)\}$, the entropy time series, where $H(t) = H(\alpha(t))$;
(2) $\{\rho_R(t)\}$, the Rohlin distances' time series $\rho_R(t) = \rho_R(\alpha(t+1), \alpha(t))$;
(3) $\{\hat{\rho}_R(t)\}$, the corresponding reduced distances;
(4) $A(t)$, the amplification factor (6);
(5) $\{\rho_H(t)\}$, the time series for the Hamming distances;
(6) $\{\bar{v}(t)\}$, the mean steepness time series $a(t)$.

We observe that, as $N$ grows, the time series $\{\bar{v}(t)\}$ is smoothed for small avalanches, but the appearance of longer and longer avalanches ensures the persistence of comparable maxima in the peaks on larger timescales. Therefore, the limit $N \to \infty$ is not trivial.

The results are as follows:

(1) To check the correctness of our simulations, standard observables $a$, $s$, $T$ and related quantities have been resumed, with the same values shown in literature [3, 8];

(2) Rohlin and Hamming distances exhibit power law distributions, likewise standard parameters (1), for both BTW and Manna automata:

$$P(\rho) \propto \rho^{-\eta} \tag{8}$$

where $\rho$ is in turn $\rho_H$, $\rho_R$ or $\hat{\rho}_R$ (see figures 1 and 2). Actual values are shown in table 1. Note that the characteristic exponents have different values for the two automata, with regards to both the Rohlin and Hamming distances.

(3) Entropy and steepness do not exhibit any power law distribution. This is easy to explain: entropy and steepness are global indicators of configuration complexity, and their distributions simply exhibit values averaged over the whole trajectory, independently of dynamical correlations (while, in contrast, correlations along the trajectory are important for distances). Entropy $H(t)$ oscillates around the mean value

$$\bar{H} = \bar{H}(N) = c \log N \tag{9}$$

where $c$ is 0.85 for BTW and 0.28 for Manna. The factor $\log N$ is typical of a 'chaotic' component, and it will be explained below. Indeed, it would be erased by normalization through the maximal Shannon entropy, $\log N$ anyway. The difference in the proportionality factor $c$, stresses some peculiarities of BTW and Manna configurations. To start with, according to the four colours theorem, a two-value alphabet cannot produce all configurations, as a four-value alphabet does. Therefore, at least in principle, Manna configurations are only a subset of BTW configurations (actually, we did not check directly the effective relevance of this possibility). This could be a source for greater complexity of the latter with respect to the former, coherent

with the observed greater factor $c$ in (9). For a deeper insight, we have explored the measure distributions of clusters for every fixed value in $K$. It results that, for both automata, clusters of value 0 *are not* distributed with a power law, but are mostly one-site islands (BTW) or few-site islands (Manna), and they are *randomly distributed*: their number is therefore proportional to $N$. This explains both the $\log N$ divergence of entropy and the difference between the two sandpiles. Once the 0-value clusters have been erased, for the Manna model there indeed remain only clusters of value 1 (with a power law distribution); for the BTW model there remain clusters of values 1, 2, 3 and they have power law distributions with different fractal dimensions (multifractality). Observe that this is another multifractality with respect to the one considered in [9].

(4) Since the values of observables are not constant for events with the same $T$, it is suitable to consider the values $\bar{a}$, $\bar{s}$, $\bar{H}$ ... averaged over all occurrences at fixed $T$. For standard parameters, these expectation values have already been considered, e.g., by [10,11]. In figure 3, we give $\bar{\rho}_R$ for BTW and Manna. The linear growth is clear for the BTW data (power with exponent $1 \pm 0.01$), while the overall growth of the Manna data presents a light concavity, allowing for a more than algebraic growth. It is true that for $T > 30$ most of the data could also be fitted by a line in the loglog scale (i.e. by a power with exponent $>1$, precisely $1.23\pm0.01$): in such case, the concavity should be interpreted as a small avalanche effect typical of the Manna system. In our opinion, such splitting of functional dependence of the mean distance versus $T$ is an additional meaningful argument supporting the idea of a class distinction between the two automata. A universality breaking given solely on the basis of table 1 would be less clear. We stress that *all* the values of $T$, not only the greater ones, must be taken into consideration. Indeed, since small avalanches remain statistically important in the limit $N \to \infty$ (the limit necessary to have indefinitely long avalanches) the possible settlement of the Manna curve in a power law growth for great $T$ does not cancel out this initial difference. In any case, at least the difference between exponents in the growth, a usual criterion to distinguish classes of universality, seems to be reliable. In figure 4 analogous diagrams for the $\rho_H$ distance give the same results with a minor emphasis on the suspected concavity of the Manna curve.

(5) The reduction process proves extremely sensitive to the rules. The amplification factors have also been averaged over all the occurrences at same $T$. Clearly, since the region not involved by the avalanche does not contribute to distances, the effective reduction has to do only with the critical region. We see from figure 5 that:

- for BTW, a quantitatively relevant amplification takes place for all $T$: to have an idea, $A$ is three orders of magnitude greater then the corresponding amplification in the critical phase of spin automata [6]. The atoms' boundaries, therefore, are very easily recovered by the internal dynamics of avalanches, also for great $T$. After an initial peak, to be attributed to the smallness of the avalanche region, there is a minimum, for $T$ of the order of 20: this is likely due to the fact that the reconstruction of borders requires sufficiently long avalanches, and this minimum simply expresses the balance between deformed and rebuilt borders. Experimentally it seems that there is a saturation of the reduction process around $T = 100$. Of course, at greater $T$ the statistics is too poor to smooth down the fluctuations;
- for Manna, the initial peak is comparable to the BTW peak, with a fast descent. For $T$ greater than 20, the randomness of the rule makes the reconstruction of borders after the avalanches extremely improbable. In this case, the amplification reduces to the order of magnitude found in spin systems.

(6) Power spectra: all distances exhibit spectra of time series with rapidly decaying correlations. The most interesting behaviours concern entropy and mean steepness: clearly,

**Table 1.** Critical exponents for distance distributions.

| Rule | $\eta_R$ | $\hat{\eta}_R$ | $\eta_H$ |
|------|----------|----------------|----------|
| BTW | $1.18 \pm 0.02$ | $1.24 \pm 0.02$ | $0.86 \pm 0.03$ |
| Manna | $1.44 \pm 0.03$ | $1.44 \pm 0.03$ | $1.49 \pm 0.03$ |

previous observation at point (3) above does not apply in this case, since in power spectra the dynamical order of events is fundamental. For the BTW automaton the entropy spectrum $S_H(\omega)$ and the mean steepness spectrum $S_{\bar{v}}(\omega)$, are shown in figures 6 and 7 respectively (Manna spectra are similar). Notwithstanding the dispersion at high frequencies, linear interpolations performed via standard numerical routines give values for critical exponents which are robust with respect to variations in the experiment parameters. Precisely, we obtain the exponent $\gamma_H = 0.82 \pm 0.05$ for BTW and $\gamma_H = 0.84 \pm 0.05$ for Manna. As for the mean steepness, we have $\gamma_{\bar{v}} = 0.75 \pm 0.05$ for BTW and $\gamma_{\bar{v}} = 0.85 \pm 0.05$ for Manna. These differences do not indicate a meaningful qualitative distinction between the two automata.

One could vary the experiments on the power spectra in two different ways:

(a) instead of instantaneous values of observables at the beginning of every avalanche, consider the values averaged during the avalanche;

(b) conversely, consider the instantaneous values also at every step within the avalanches and between them.

Actually, we have performed both these variations with $L = 50$, obtaining practically identical results with respect to the standard experiments.

*Conclusions*

The last result for critical exponents from the power spectra of entropy and steepness (i.e., their independence of the timing in the sampling, or else of the local averaging during the avalanches) is a strong indication about the special character of the SOC noise in its relation to fractality: cluster complexity and local steepness indeed vary in such a way to pass through the total length of avalanches as if it were a single evolution step; in addition, the averaging along the avalanches does not destroy the fluctuations. In other words, zooming in on time series by looking at intermediate evolution steps, gives new similar time series, etc.

Introducing the Hamming and Rohlin distances, we have remarked upon their complementarity: the former refers to the local (site by site) difference of values and needs a numerical (or metrizable) alphabet; the latter refers to the global cluster distribution and it is indifferent to the nature of the alphabet (which could also consist of colours or letters), exploiting only shapes and sizes of clusters. The relation of both to dynamics should, in principle, point to different features. However, we did not, in fact, obtain qualitatively different information from $\rho_H$ or $\rho_R$. Such an experimental result has to be interpreted as an indication that dynamics and geometry are interlaced in such a way that not only cluster variations imply changes of local values, but also that local variations imply shape evolution (and this is not necessarily true). Such a feature does not regard only sandpile dynamics, but it is true for all rules in which there is an interdependence between evolution and cluster borders (e.g. in Q2R spin system [6]). Of course, the Hamming distance cannot provide information about the factorization of partitions, as the Rohlin distance does.

These features do not distinguish between BTW and Manna rules. As far as we know, they may be considered as typical of SOC in itself.
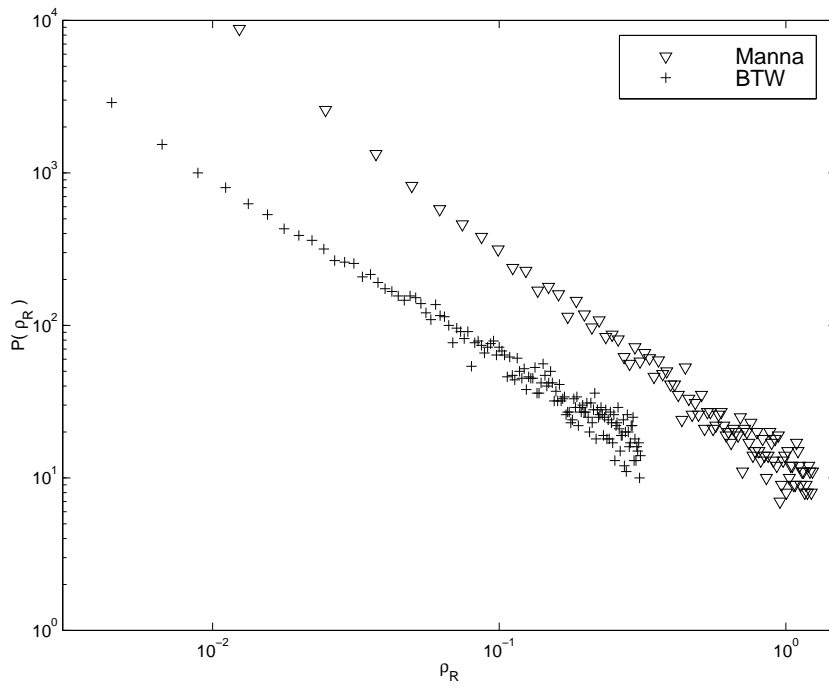
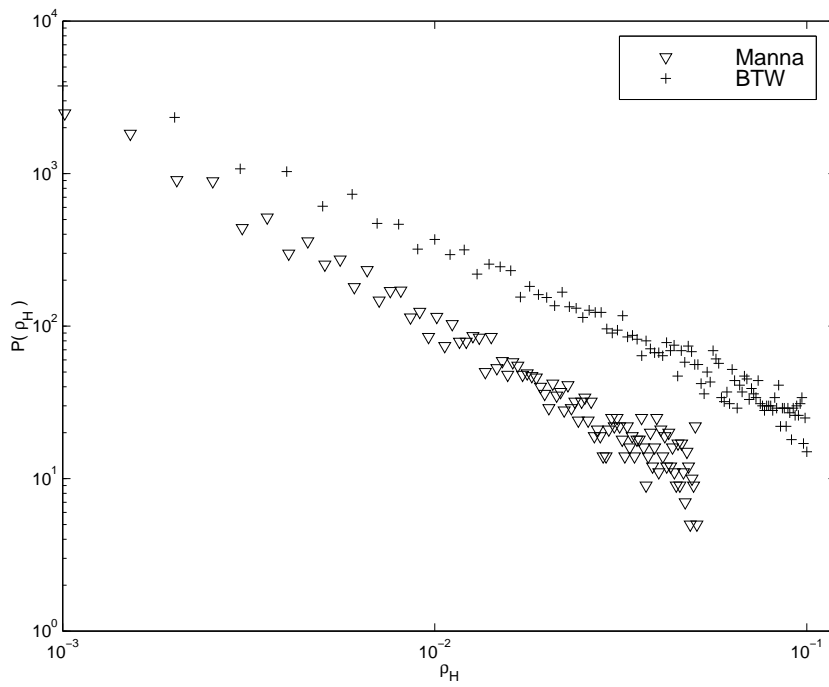**Figure 1.** Distributions of Rohlin distances for BTW and Manna automata.



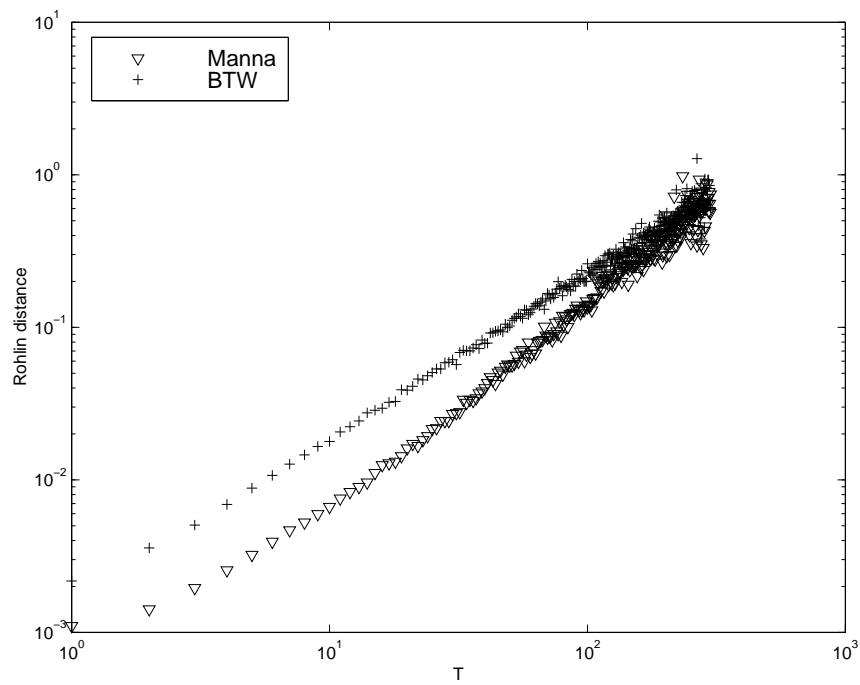**Figure 2.** Distributions of Hamming distances for BTW and Manna automata.

**Figure 3.** Mean Rohlin distances as a function of lifetime $T$. Averages are over all occurrences at fixed $T$.
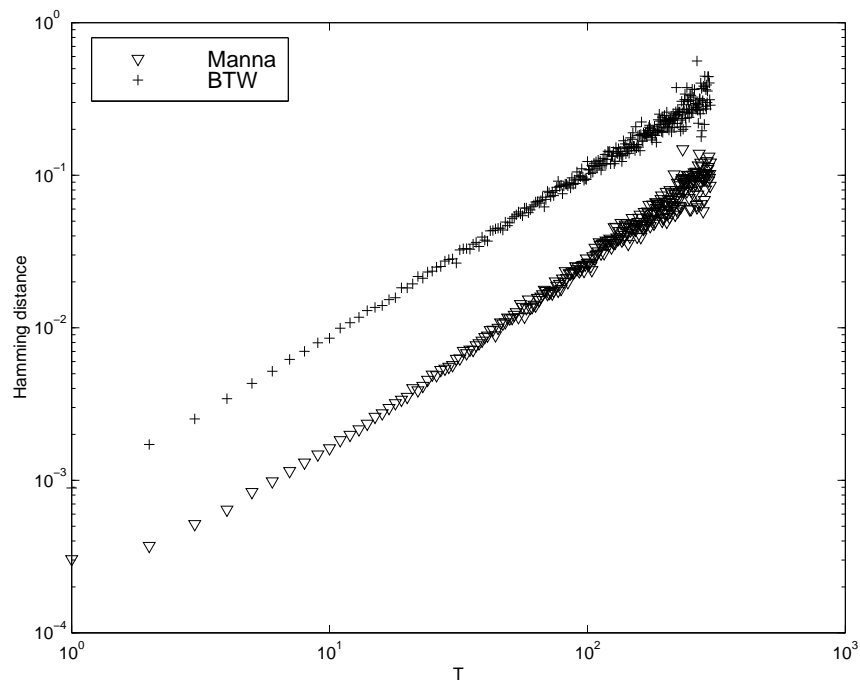


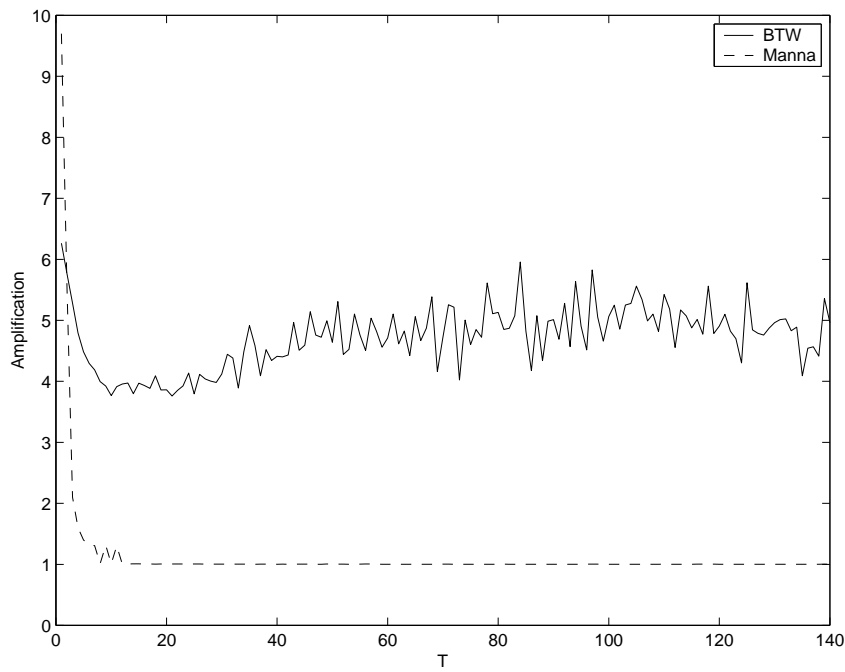**Figure 4.** The same as in figure 3 but for Hamming distances.

**Figure 5.** Mean amplification factor $\bar{A}$ versus $T$, for BTW (full curve) and Manna (dashed curve) systems. Averages as in figure 3.
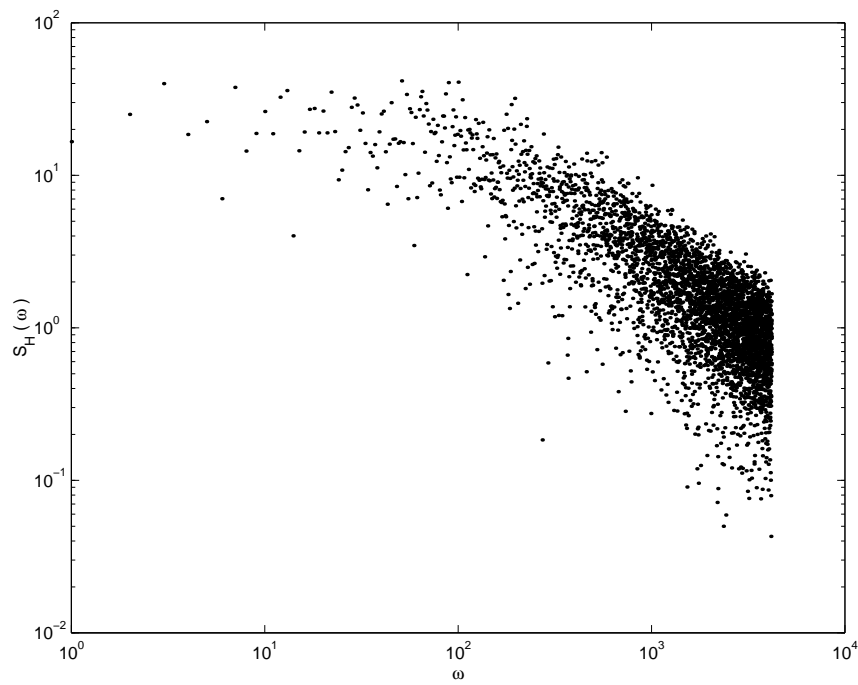


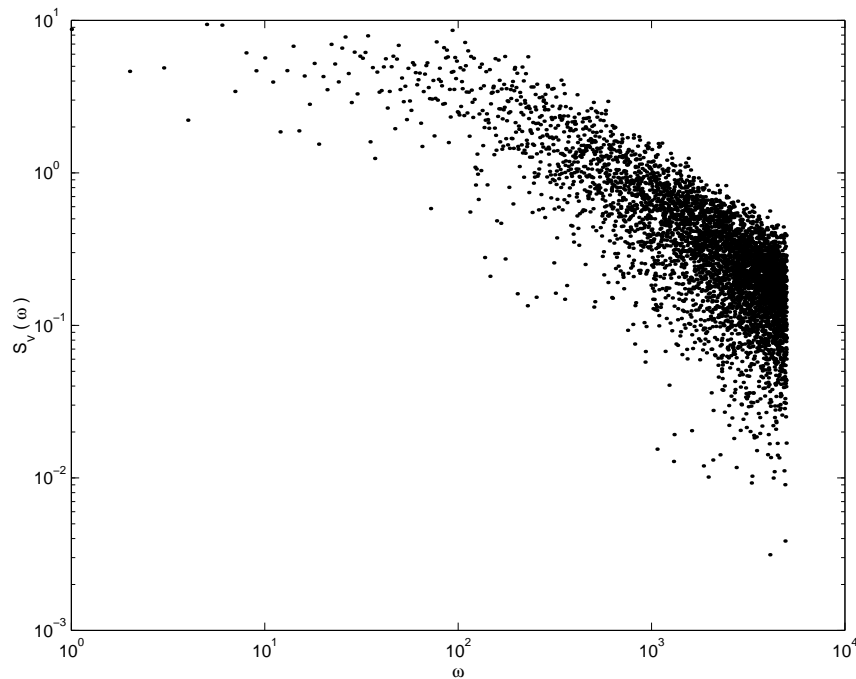**Figure 6.** Power spectrum of Shannon $H$ entropy for BTW automaton.

**Figure 7.** Power spectrum of steepness $\bar{v}$ for BTW automaton.

Finally, stochasticity in Manna rule is likely to be responsible for its greater growth law of a Rohlin distance at fixed lifetime $T$ (figure 3) and extremely low reduction with respect to BTW (figure 5). All this shows that common features of SOC states may coexist with deeply different properties in the time correlations of configurations. These findings provide strong indication regarding a possible split of the universality class for the two automata, which was not clear from previously considered parameters.

## References

[1]  Bak P, Tang C and Wiesenfeld K 1987 *Phys. Rev. Lett.* **59** 381
     Bak P, Tang C and Wiesenfeld K 1988 *Phys. Rev.* A **38** 364–74
[2]  Manna S S 1991 *J. Phys. A: Math. Gen.* **24** L363–9
[3]  Chessa A, Stanley H E, Vespignani A and Zapperi S 1999 *Phys. Rev.* E **59** R12
[4]  Martin N F G and England J W 1981 *Mathematical Theory of Entropy* (Reading, MA: Addison-Wesley)
[5]  Casartelli M 1990 *Complex Syst.* **4** 491–507
     Albrigi A and Casartelli M 1993 *Complex Syst.* **7** 171–97
[6]  Bettati D, Casartelli M, Celli P and Malpeli L 1998 *J. Phys. A: Math. Gen.* **31** 9359–76
[7]  Peierls R 1936 *Proc. Camb. Phil. Soc.* **32** 477
     Griffith R B 1964 *Phys. Rev.* A **136** 537
[8]  Manna S S 1990 *J. Stat. Phys.* **59** 509
[9]  Tebaldi C, De Menech M and Stella A 1999 *Phys. Rev. Lett.* **83** 3952
[10] Christensen K and Zeev Olami 1993 *Phys. Rev.* E **48** 3361–72
[11] Ben-Hur A and Biham O 1996 *Phys. Rev.* E **53** R1317–20